Polymerization in Nanometer-Sized Fibers: Molecular Packing Order and Polymerizability

Mitsutoshi Masuda,* Takeshi Hanada,† Yuji Okada, Kiyoshi Yase, and Toshimi Shimizu

National Institute of Materials and Chemical Research, 1-1 Higashi, Tsukuba, Ibaraki 305-8565, Japan

Received July 5, 2000; Revised Manuscript Received October 15, 2000

ABSTRACT: The bolaform 1-glucosamide **1** and its deacetylated derivative **2** (*N*,*N*′-bis(2,3,4,6-tetra-*O*-acetyl-*β*-D-glucopyranosyl)deca-4,6-diyne-1,10-dicarboxamide and *N*,*N*′-bis(*β*-D-glucopyranosyl)deca-4,6-diyne-1,10-dicarboxamide, respectively) have been synthesized and their self-assembled structures investigated. The hydrophobic peracetylated derivative **1** formed an organogel from solution in boiling ethyl acetate/*n*-hexane mixtures on cooling to room temperature. In contrast, **2** produced fibrous assemblies from aqueous solution on addition of THF via vapor diffusion. Energy filtering transmission electron microscopy (EF-TEM) revealed the formation of nanometer-sized fibers (nanofibers) with widths of between 6 and 20 nm and more than 50 nm for **1** and **2**, respectively. The amide and sugar hydroxyl groups in **2** allow formation of stronger, multiple hydrogen bond networks in the nanofiber than for **1**. Powder X-ray diffraction studies revealed that fibers derived from **2** displayed a higher molecular packing order than those from **1**. Exposure of a dispersion of either nanofiber to UV light resulted in the appearance of a red coloration. While the UV-irradiated nanofibers of **1** were readily soluble in $CHCl_3$, those of **2** required peracetylation to allow dissolution. Subsequent gel permeation chromatography for the UV-irradiated nanofibers displayed peak-top molecular weights corresponding to 13-mer and 64-mer for **1** and **2**, respectively. On the basis of EF-TEM observation, no significant morphological changes in the fibers were found after UV-initiated polymerization. On the basis of these findings, we suggest that the polymerization proceeds efficiently within the nanofiber morphologies with higher molecular packing order leading to a higher degree of polymerization to give *π*-conjugated polymer chains.

Introduction

The incorporation of polymerizable moieties into self-assembling molecules and the subsequent polymerization in the assemblies enables the stabilization of the resultant architectures with covalent linkages.[1] The diacetylene moiety is just such a polymerizable group which not only enables this stabilization but also provides information on the molecular ordering within the assemblies,[2] since the diacetylene polymerization is known to require strict structural alignments.[3] While many studies have been reported on the polymerization of diacetylene in self-assembled morphologies,[3,4] to date no direct evidence has been presented concerning the relationship between molecular packing order in the assembly and polymerizability. This is because (except-for a few cases[5,6]) the insoluble nature of most polydiacetylenes impedes further characterization of the polymeric structures formed.

We recently demonstrated self-assembled nanometer-sized fiber (nanofiber) formation and polymerization of the nanofibers from diacetylenic bolaform tetraacetyl-1-glucosamide **1**.[7] The headgroup interaction between molecules is enhanced for **2** (obtained by deprotection of the tetraacetyl group of the 1-glucosamide headgroup) since both amide and sugar hydroxyl groups are present and allow formation of stronger, multiple hydrogen bond networks. Here we describe the self-assembling behavior and polymerization of the nanofibers from hydrophobic monomer **1** and amphiphilic homologue **2**. On the basis of X-ray powder diffraction studies and molecular weight analysis of the polymerized nanofibers, we discuss the relationship between the molecular packing order in the self-assembled nanofibers and their obtained degree of polymerization.

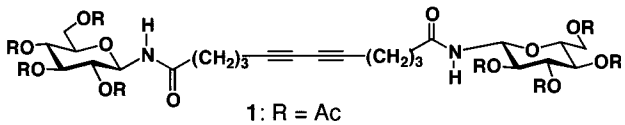

1: R = Ac
2: R = H

Experimental Section

Materials. The polymerizable bolaform (**1**) and bolaamphiphilic 1-glucosamide (**2**) with 100% *β*-configuration were synthesized by condensation of 2,3,4,6-tetra-*O*-acetyl-*β*-D-glucopyranosylamine with 5,7-dodecadiynedioic acid dichloride followed by deacetylation.[8] To avoid thermal polymerization, we converted 5,7-dodecadiynedioic acid into the corresponding diacid dichloride using oxalyl chloride.[9]

Preparation of 5,7-Dodecadiynedioic Acid Dichloride. 5,7-Dodecadiynedioic acid (3.6 mmol) purchased from GFS Chemicals was dissolved in an EtOH/THF (5 mL/5 mL) mixture. To this solution was added an ethanolic NaOH solution (7.2 mmol/5 mL) at room temperature. After stirring for 5 min, the solvent was evaporated and the residue dried in a vacuum for 6 h. To the reaction residue were added diethyl ether (10 mL), DMF (one drop), and oxalyl chloride (32 mmol) at 0 °C. After stirring for 2 h, the dispersion was filtered, and the obtained filtrate was concentrated by evaporation. The residue was used for the condensation reaction without purification.

Octaacetylated Derivative 1. The reaction mixture was purified by column chromatography. Elution with a $CHCl_3$/methanol (MeOH) mixture (gradient elution from 1% to 8% MeOH vs $CHCl_3$) gave a pure octaacetylated derivative **1**.

† Present address: The Institute of Scientific and Industrial Research, Osaka University, 8-1 Mihogaoka, Ibaraki, Osaka 567-0047, Japan.

10.1021/ma001157e CCC: $19.00
Published on Web 11/23/2000

Cooling of a hot solution of ethyl acetate (EtOAc)/*n*-hexane (1:3, v/v) afforded **1** as an organogel.

Deacetylated Derivative 2. Deacetylation of the compound **1** was carried out according to the method reported previously.[8] The details of the analytical data for the compounds **1** and **2** are available in the Supporting Information.

Compound **1** is freely soluble in wide variety of polar organic solvents, such as EtOAc, THF, $CHCl_3$, and MeOH, while **2** is only soluble in highly polar solvent, such as H_2O, DMF, and DMSO.

Nanofiber Self-Assembly. The hydrophobic 1-glucosamide **1** (0.6 g) was dissolved in EtOAc (30 mL)/*n*-hexane (70 mL) at reflux. Fibers were formed as an organogel when the boiling solution was gradually cooled to room temperature (cooling rate: −5 °C/min). To avoid the resolubilization of the self-assemblies, we added *n*-hexane (200 mL) to the solution. The amphiphilic 1-glucosamide **2** (46 mg) was dissolved in H_2O (8 mL). THF (40 mL) was slowly added by vapor diffusion at 20 °C. A fibrous assembly was obtainable over a period of several days. The resulting fibers were also diluted with THF (32 mL) to avoid redissolution.

Polymerization of Nanofibers. UV irradiation of the self-assembled nanofibers from **1** and **2** was carried out in a quartz reaction tube (1 cm path length, 20 mL volume) using a 110 W low-pressure Hg lamp (254 nm) under an argon atmosphere. The lamp-to-cell distance was fixed to 10 cm. The photoreactor was equilibrated for 20 min prior to use with the temperature maintained at 20 °C. Conversion to the polymerized nanofibers of **1** and **2** was monitored by extraction of the unreacted monomers with MeOH and H_2O, respectively.

Acetylation of Polymerized Nanofiber of 2. Acetylation of the sugar hydroxyl groups in the polymerized nanofibers was carried out according to the method previously reported for acetylation of cotton fabrics.[10] A mixture of H_2SO_4 (0.1 mL) and acetic anhydride (9.9 mL) was heated at 95 °C for 10 min. After cooling to room temperature, the mixture (10 mL) was diluted with CH_2Cl_2 (56 mL). The polymerized fibers (10.4 mg) were dispersed in 10 mL of this solution. The fibrous dispersion became a yellow homogeneous solution within 30 min. After stirring for 2 h the solution was washed with 5 wt % aqueous $NaHCO_3$ solution followed by H_2O. The organic layer was dried over anhydrous Na_2SO_4, filtrated, and concentrated. The acetylation conversion was estimated from the integration ratio of the acetyl and C-1−C-4 glucosamide ring proton signals in the ^1H NMR spectrum. Recovery of the acetylated **2** after the reaction: 95% and the conversion estimated from ^1H NMR: 92%. The more common method using acetic anhydride in pyridine was unsuccessful even in the presence of DMSO, DMF, and $CHCl_3$.

FT-IR. IR spectra were collected using a Fourier transform (FT) spectrometer (JASCO FT-620 and Micro-20/FT/IR-620) operating at 2 cm^{-1} resolution with an unpolarized beam striking the sample at normal incidence.

Molecular Weight Analysis. Gel permeation chromatography (GPC) analysis was carried out using a Shimadzu Class-LC10 system with a Shodex K-805L column using $CHCl_3$ as an eluent at 40 °C. UV absorption at 462 nm was monitored for all measurements.

Energy Filtering Transmission Electron Microscopy (EF-TEM). Unstained specimens for electron microscopy were prepared by placing three drops of the nanofiber dispersion on an amorphous carbon supporting film or polystyrene casted mesh film mounted on a standard TEM grid. The drops were then blotted off with filter paper. The dried specimens were examined by electron spectroscopic imaging using an electron microscope (Carl Zeiss EM902) operated at 80 keV with Castain-Henry type electron energy filtering at room temperature. Zero-loss bright field images were recorded on an imaging plate (Fuji Photo Film Co., Ltd. FDL5000) with a 20 eV energy windows at 3000−250000× and digitally enlarged.

Powder X-ray Diffraction (XRD) Measurement. All powder patterns were taken by the reflection method with a Rigaku RINT-2100 powder diffractometer (50 kV and 40 mA). The Cu Kα beam was taken out using a graphite monochromator. The spectra were measured at room temperature between 1° and 36° in the $2\theta/\theta$ scan mode with steps of 0.01° in 2θ and 0.6 s measurement time per step.

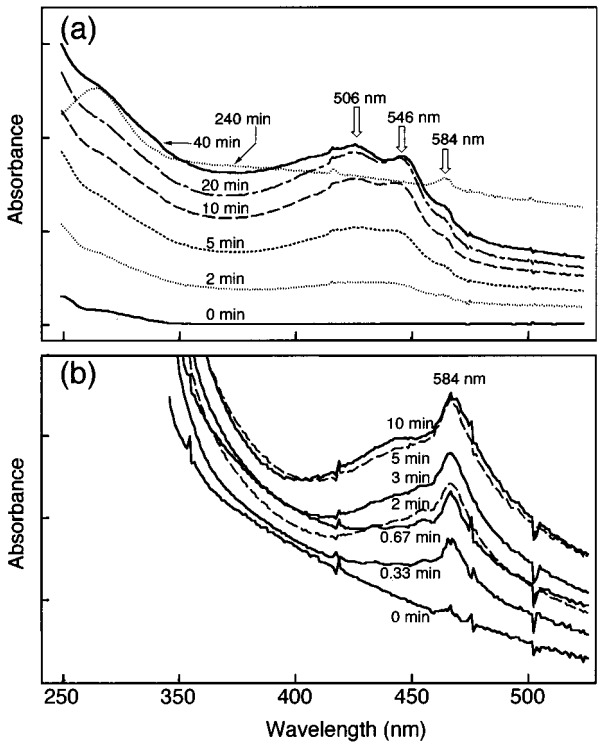

Figure 1. UV−vis absorption spectra for suspensions of (a) nanofibers derived from **1** in EtOAc/*n*-hexane (1:9, v/v) and (b) nanofibers derived from **2** in H_2O/THF (1:9, v/v).

Results and Discussion

Self-Assembly and Polymerization of Nanofibers from 1. On slow cooling to room temperature, solutions of **1** in a boiling EtOAc/*n*-hexane mixture (3/7, v/v) solidified to form an organogel. The critical gel concentration of **1** at 20 °C was 4.0 g/L for EtOAc/*n*-hexane mixture (1/3, v/v). Similar gelation has also been found to occur for saturated chain bolaform 1-glucosamides[8] and urethane amides.[11] No gels of **1** were observed when polar organic solvents such as MeOH, $CHCl_3$, and DMF were used. Exposure of a gel dispersion of **1** in an EtOAc/*n*-hexane mixture (1/9, v/v) to 254 nm light or γ-ray under an argon atmosphere resulted in the appearance of a red coloration, with the optimal UV irradiation period determined to be 40 min on the basis of UV−vis spectral changes (Figure 1a). Further irradiation (240 min) induced hypochromism from red to orange, which suggests decomposition or shortening of π-conjugated chains.

Characterization of Nanofibers from 1. EF-TEM revealed that the self-assembled gel of **1** with mixture of EtOAc/*n*-hexane was composed of nanometer-sized fibers (nanofibers) with widths of between 6 and 20 nm (Figure 2a,b). The minimum width (6 nm) corresponds to twice the molecular length of an extended monomer **1** (3.05 nm). Images obtained of partial twisting of the nanofibers from **1** suggested that the fibers are flexible ribbons (Figure 2b). The nanofibers of **1** were robust during the EF-TEM observation, presumably due to partial polymerization of the diacetylenes by the electron beam. No fibrous morphology of **1** was observed via TEM examination of solutions at concentrations lower than the critical gel concentration.

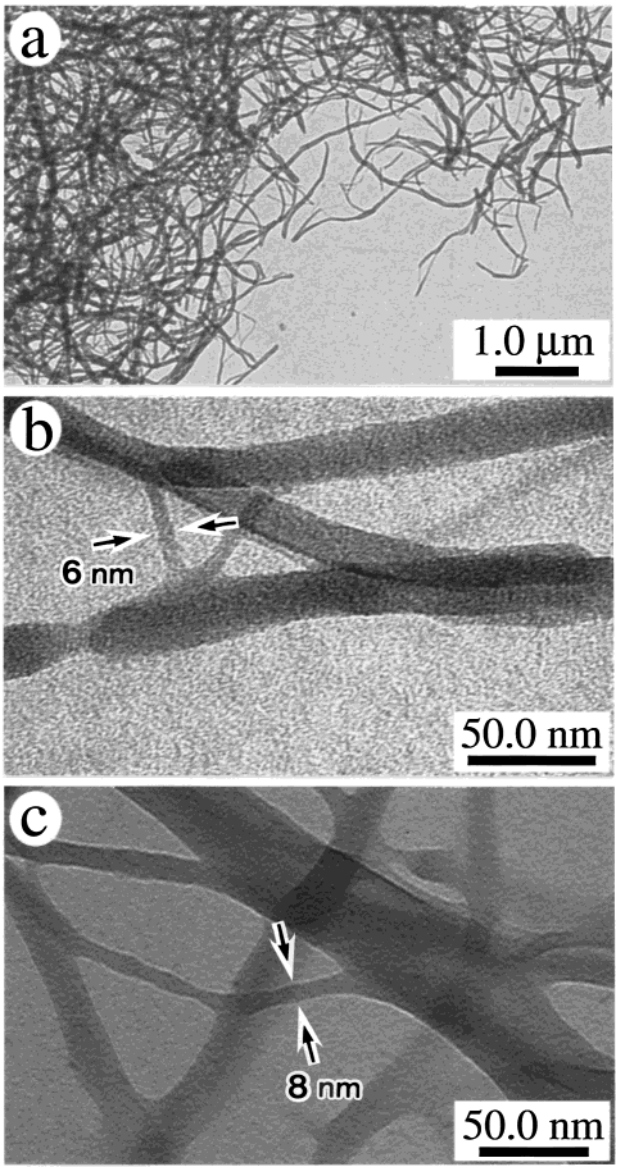

Figure 2. EF-TEM images of (a, b) the self-assembled nanofibers derived from **1** in EtOAc/*n*-hexane (1:9, v/v) (dried and unstained) and (c) the polymerized nanofibers following UV irradiation (40 min) in EtOAc/*n*-hexane (1:9, v/v).

EF-TEM observation of the polymerized nanofibers of **1** revealed a fibrous morphology similar to those observed before irradiation (Figure 2c), indicating that the polymerization proceeds within the individual nanofibers. The minimum width of the polymerized nanofibers of **1** was found to be slightly extended to 8 nm, corresponding to 2 or 3 times an extended molecular length (3.05 nm). Nanofibers polymerized by γ-ray irradiation also showed similar widths and morphologies.[7]

IR spectroscopic investigation of the self-assembled nanofibers from **1** gave N−H stretching (3343 cm^{-1}), amide I (1680 cm^{-1}), and amide II band (1535 cm^{-1}) frequencies which all support the formation of amide hydrogen bonds within the nanofibers (Figure 3b), in a fashion similar to that of other bolaform amide gelators.[11] In contrast, a dried amorphous sample of **1** obtained from $CHCl_3$ solution was found to display no such evidence of hydrogen bonds between amide groups (Figure 3a). Thus, the formation of amide hydrogen bonds directs the self-assembly and resultant nanofiber formation from **1**.

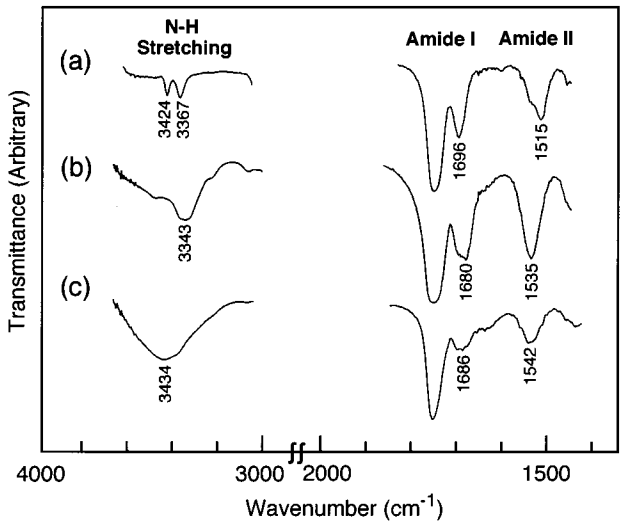

Figure 3. FT-IR spectra of **1**: (a) an amorphous film obtained from $CHCl_3$ solution, (b) the self-assembled nanofibers in EtOAc/*n*-hexane (1:9, v/v), and (c) the polymerized nanofibers in EtOAc/*n*-hexane (1:9, v/v).

Self-Assembly and Polymerization of Nanofibers from 2. The 1-glucosamide bolaamphiphile **2** was highly soluble in H_2O (≈50 wt %), and self-assembly to form fibers did not occur under similar conditions to those previously reported for the analogous 1-glucosamide derivatives with a saturated oligomethylene chain of the same carbon number.[12] Thus, we added a poor solvent (THF) to the aqueous solution using vapor diffusion method to induce self-assembly. The fibrous assemblies appeared when vol % concentration of H_2O became less than 20% against THF at 20 °C. The UV-initiated polymerization (254 nm) of the nanofibers from **2** was found to be complete in only 10 min (Figure 1b). The λ_{max} (584 nm) of the polymerized nanofibers was of longer wavelength than that of **1** (506 and 546 nm). In addition, cast films of **2** obtained from aqueous solution changed color upon UV irradiation, while those of **1** (from $CHCl_3$ solution) gave no color change. This difference can be explained in term of the presence of relatively stronger intermolecular interactions for **2**.

Characterization of Nanofibers from 2. The EF-TEM observation of the fibrous assemblies from **2** showed fiber or needle morphologies with a minimum width of 50 nm, much larger than those found in fibers derived from **1** (6 nm) (Figure 4a). The self-assembled nanofibers seem rigid and brittle. UV polymerization of nanofibers derived from **2** proceeded with retention of the fiber morphology (Figure 4b), in a manner similar to that already described. While the polymerized nanofibers seemed robust and flexible under TEM observation, care was required during sample preparation since self-assembled nanofibers of **2** is hygroscopic and can easily dissolve in condensed H_2O. The minimum width of irradiated nanofibers derived from **2** was approximately 20 nm, which is bigger than those derived from **1**, presumably due to enhanced interlayer interactions.

Figure 5 shows FT-IR spectra of the self-assembled and polymerized nanofibers of **2**. The lower frequency shift of the N−H stretching, amide I, and amide II bands strongly suggests that the amide hydrogen bonds within the nanofibers derived from **2** are stronger than those already described for **1** (Figures 3a and 5a). The sugar hydroxyl groups in **2** can also form hydrogen bonds, as seen between the 1-glucosamide headgroups of the

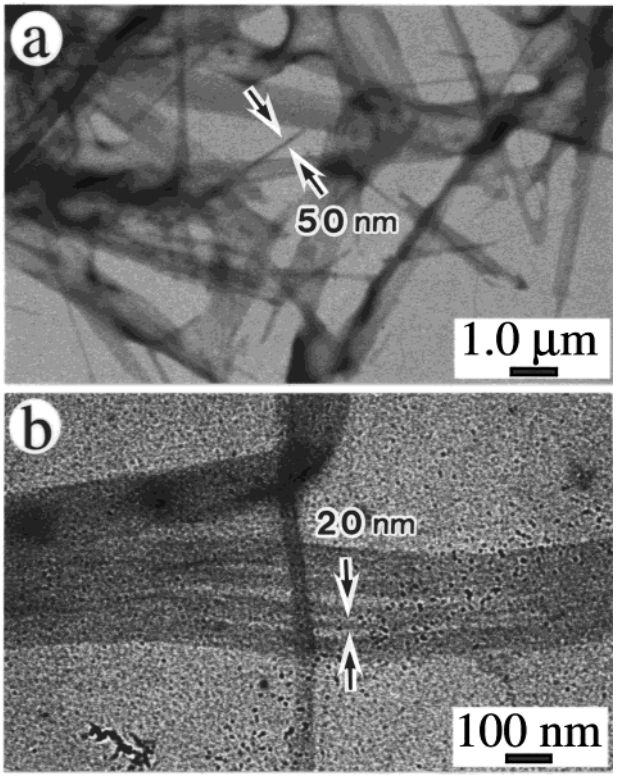

Figure 4. EF-TEM images of (a) the self-assembled nanofibers derived from **2** in H_2O/THF (1:9, v/v) (dried and unstained) and (b) the UV-polymerized nanofibers (5 min) in H_2O/THF (1:9, v/v).

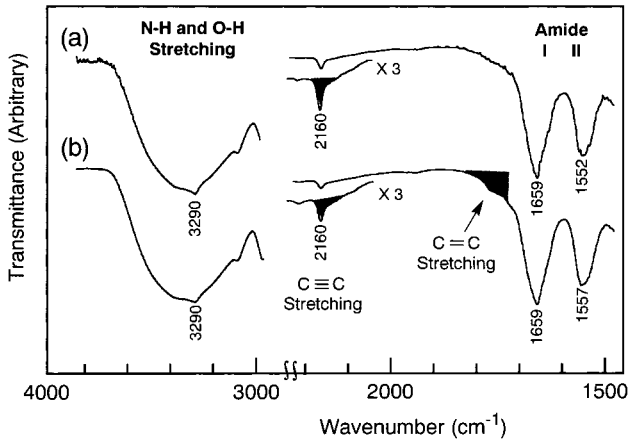

Figure 5. FT-IR spectra of the nanofibers from **2** (a) before and (b) after UV irradiation (10 min).

analogous saturated-chain bolaamphiphile previously reported,[13] although the broadening of the O−H stretching band around 3600−3200 cm^{-1} prevents a more quantitative analysis. No remarkable frequency shifts of the N−H stretching, amide I, and amide II bands were observed between the self-assembled and polymerized nanofibers from **2**, in contrast to the large frequency shifts seen for those from **1**. This means that the molecular packing in the nanofibers of **2** is more suitable for the polymerization than that in the nanofibers of **1**.

The appearance of the C≡C stretching band around 2160 cm^{-1} for the self-assembled nanofibers from **2** indicates unsymmetric packing of the molecules within the nanofibers since in general, no such band absorption is observed for symmetric diacetylenic molecules.[14] After irradiation, a reduction in intensity of the C≡C stretching band (73% in absorption spectra) and the appearance of the FT-IR shoulder for C=C double bonds (1725−1740 cm^{-1} as shown in Figure 5) both support the proposed polymerization of **2** within the nanofibers.

Table 1. Characteristics of the Self-Assembled Nanofibers

monomer	solvent for self-assembly	*d*-spacing[a] (nm)	molecular length[b] (nm)	tilt angle[c] (deg)
1	AcOEt/*n*-hexane (3/7)	n.d.[d]	3.05	n.d.[d]
2	H_2O/THF (1/5)	2.22	2.71	40

[a] Observed from XRD peaks in the small-angle region. [b] Values estimated from an extended molecular model. [c] Tilt angle of the hydrophobic chain was estimated from the molecular length and *d*-spacing from XRD. [d] Not determined.

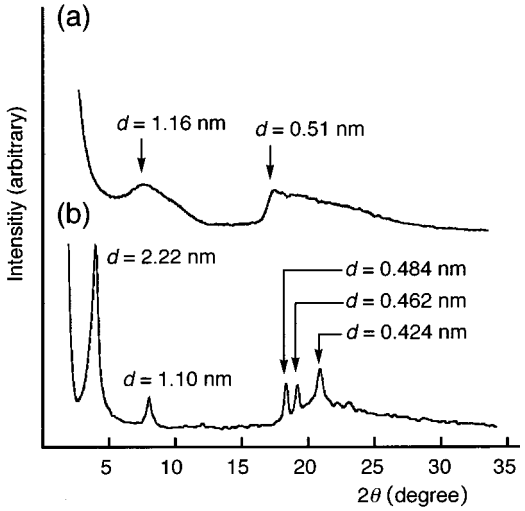

Figure 6. Powder XRD spectra of the self-assembled nanofibers (a) from **1** and (b) from **2**.

XRD Measurement. To investigate the molecular packing, we measured the powder XRD pattern of the self-assembled nanofibers (Figure 6a,b). Table 1 summarizes the *d*-spacings found for dried nanofibers (with corresponding molecular lengths calculated assuming an extended conformation) and highlights the difference in molecular packing order found when comparing the self-assembled nanofibers derived from **1** and **2**. All diffraction peaks of the nanofibers from **2** are sharp and indicate highly ordered layer packing similar to that previously reported for saturated-chain aldosamide bolaamphiphiles.[12,13,15] In contrast, the broad diffraction peaks of the nanofibers from **1** suggest a lower molecular packing order (Figure 7) arising as a consequence of the weaker intermolecular interactions in **1** when compared with **2**. The absence of peaks arising from layered structures in the small-angle region (the 1.16 nm spacing for the nanofiber of **1** corresponds to the width of the tetraacetyl 1-glucosamide headgroup) is presumably due to low interlayer molecular interactions within the nanofibers of **1**. The flexible and thin nanofiber obtained from saturated chain 1-glucosamide bolaamphiphiles gave a similar weak diffraction in the small-angle region of the XRD pattern.[12]

It has been well documented that macromonomers incorporating diacetylene units can polymerize readily in crystalline domains[16] with the polymerizability strongly dependent on the packing parameters.[3] Considering such strict positional requirement, the butadiene units seem to align at a critical repeat distance near 5.0 Å with an orientation angle of about 45°

Table 2. Characteristics of the Polymerized Nanofibers

	irradiation		polymerized nanofibers			
monomer	solvent	time (min)	conversion[a] (%)	λ_{max}[b] (nm)	M_n[c]	M_w/M_n
1	AcOEt/*n*-hexane (1/9)	40	32	506, 546	1.10×10^4	2.4
1	AcOEt/*n*-hexane (1/9)	240	20	n.d.[d]	1.06×10^4	2.5
2	H_2O/THF (1/9)	10	27	584	5.65×10^4	2.2

[a] Determined by extraction of the unreacted monomers from the polymerized nanofibers. [b] λ_{max} of UV-irradiated nanofiber dispersion in corresponding solvent. [c] Absorbance was monitored at 460 nm. [d] Not determined.

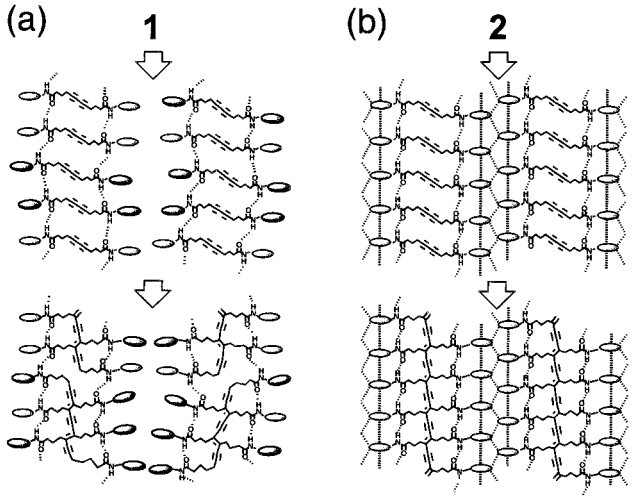

Figure 7. Schematic illustration of the molecular packing order in the self-assembled and polymerized states (a) **1** from EtOAc/*n*-hexane and (b) **2** from H_2O/THF.

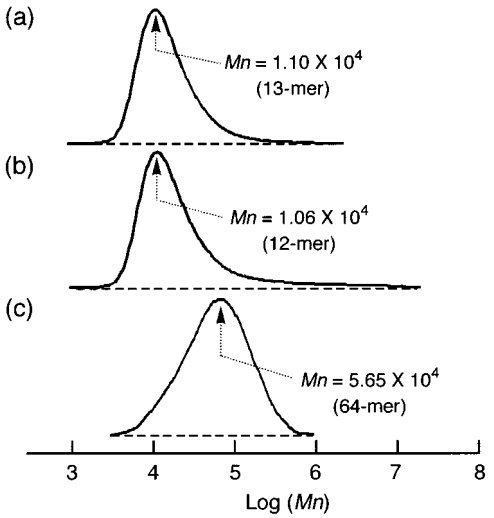

Figure 8. Molecular weight distribution of the polymerized nanofibers against a polystyrene standard: (a) 40 min and (b) 240 min irradiation for **1** in EtOAc/*n*-hexane (1:9, v/v) and (c) 10 min irradiation of **2** in H_2O/THF (1:9, v/v) with subsequent per-acetylation. Absorbance was monitored at 462 nm. Solvent: $CHCl_3$.

relative to the translation axis within the nanofibers from **1** or **2**.

Acetylation of Polymerized Nanofibers Derived from 2. Gel permeation chromatography (GPC) measurements for **1** were made using chloroform as the eluent of choice, since both pre- and postpolymerization fibers were found to be readily soluble. On the other hand, the polymerized nanofibers derived from **2** were found to be completely insoluble in most common solvents, including hot DMSO, DMF, and H_2O. This property provides strong evidence for efficient polymerization but makes it difficult to analyze the molecular weight of the polymerized fibers in the manner already described.

With this in mind, acid-catalyzed acetylation of the sugar hydroxyl groups was carried out for the polymerized nanofibers derived from **2**.[10] The acetylation proceeded with a 95% yield, quite high in comparison with the reported cotton fiber acetylation (75% yield)[10] presumably due to the lower steric hindrance of the sugar moieties as a side chain. ^{1}H NMR and FT-IR spectra of the acetylated polymeric nanofibers of **2** were identical to those derived from **1**.

Molecular Weight Analysis. GPC analysis of the UV-irradiated nanofibers provided definitive evidence of their polymerization (Figure 8a−c), and Table 2 summarizes the polymerization data, including calculated number-average molecular weight and polydispersity values (M_n and M_w/M_n, respectively) using a polystyrene standard. The 462 nm absorbance was monitored since it corresponds to the λ_{max} of all nanofiber solutions in $CHCl_3$.[6] The GPC profile of nanofibers derived from **1** after 40 min of irradiation showed a peak top at 1.1×10^4, corresponding to a 13-mer (Figure 8a). A similar distribution was found after 240 min of irradiation (Figure 8b), although small amounts of higher molecular weight components (presumably due to cross-linkage) also appeared and the low calculated conversion and hypochromism suggested degradation of the nanofibers (Table 2). The polymerized nanofibers of **2** gave a relatively higher peak top than those of **1**, corresponding to the formation of a 64-mer (Figure 8c). Remarkably, the obtained degree of polymerization reflects the degree of molecular packing order within each self-assembled nanofibers (Figure 7a,b). The self-assembled nanofibers with high molecular packing order, such as **2**, result in higher degree of polymerization (Figure 7b). The less ordered nanofibers such as **1** gave relatively lower degree of polymerization (Figure 7a). These degrees of polymerization are, however, 2 orders lower in magnitude than that of general solid-state polymerized diacetylenes.[5,6]

Conclusion

Diacetylene 1-glucosamides **1** and **2** self-assembled to form nanofibers from free solution. Linear amide hydrogen bond formation directed the nanofiber self-assembly of **1**, with self-assembled nanofibers derived from **2** additionally stabilized by multiple hydrogen bonds between sugar hydroxyl groups and amide groups. This higher molecular packing order within the nanofibers derived from **2** produced relatively higher molecular weight polydiacetylene following UV polymerization as confirmed by GPC analysis after solubilization of the polydiacetylenic nanofibers of **2** via acetylation of the sugar hydroxyl groups.

Supporting Information Available: Text giving details of the analytical data for the monomers **1** and **2**. This material

is available free of charge via the Internet at http://pubs.acs.org.

References and Notes

(1) (a) Fuhrhop, J.-H.; Köning, J. *Membranes and Molecular Assemblies: The Synkinetic Approach*, 1st ed.; The Royal Society of Chemistry: Cambridge, UK, 1994. (b) Lin, G. In *Polymeric Nanostructures*; Nalwa, H. S., Ed.; *Handbook of Nanostructured Materials and Nanotechnology*; Academic Press: New York, 2000; Vol. 5, pp 475−500. (c) Lin, G.; Qiao, L.; Guo, A. *Macromolecules* **1996**, *29*, 5508−5510. (d) Stewart, S.; Lin, G. *Angew. Chem., Int. Ed. Engl.* **2000**, *39*, 340−344.

(2) Frankel, D. A.; O'Brien, D. F. *J. Am. Chem. Soc.* **1994**, *116*, 10057−10069.

(3) (a) Wegner, G. *Makromol. Chem.* **1972**, *154*, 35−48. (b) Bassler, H.; Enkelmann, V.; Sixl, H. *Advances in Polymer Science*; Springer-Verlag: Berlin, 1984; Vol. 63.

(4) (a) Ringsdorf, H.; Schlarb, B.; Venzmer, J. *Angew. Chem., Int. Ed. Engl.* **1988**, *27*, 113−158. (b) Tieke, B.; Wegner, G. *Topics in Surface Chemistry*; Kay, E., Bagus, P. S., Eds.; Plenum Press: New York, 1978; pp 121−134. (c) O'Brien, D. F.; Whitesides, T. H.; Klingbiel, R. T. *J. Polym. Sci., Polym. Lett. Ed.* **1981**, *19*, 95−101. (d) Fuhrhop, J.-H.; Blumtritt, P.; Lehmann, C.; Luger, P. *J. Am. Chem. Soc.* **1991**, *113*, 7437−7439. (e) Kim, T.; Chan, K. C.; Crooks, R. M. *J. Am. Chem. Soc.* **1997**, *119*, 189−193. (f) Georger, J. H.; Singh, A.; Price, R. R.; Schnur, J. M.; Yager, P.; Schoen, P. E. *J. Am. Chem. Soc.* **1987**, *109*, 6169−6175. (g) Svenson, S.; Messersmith, P. B. *Langmuir* **1999**, *15*, 4464−4471. (h) Inoue, K.; Ono, Y.; Kanekiyo, Y.; Hanabusa, K.; Shinkai, S. *Chem. Lett.* **1999**, 429−430.

(5) Patel, G. N.; Walsh, E. K. *J. Polym. Sci., Polym. Lett. Ed.* **1979**, *17*, 203−208.

(6) Wenz, G.; Wegner, G. *Makromol. Chem., Rapid Commun.* **1982**, *3*, 231−237.

(7) Masuda, M.; Hanada, T.; Yase, K.; Shimizu, T. *Macromolecules* **1998**, *31*, 9403−9405.

(8) Masuda, M.; Shimizu, T. *J. Carbohydr. Chem.* **1998**, *17*, 405−416.

(9) Beeby, P. J. *Tetrahedron Lett.* **1977**, *38*, 3379−3382.

(10) Tuji, W.; Kitamaru, R.; Sakaguchi, Y. *Sen'i Gakkaishi* **1960**, *16*, 1020−1018.

(11) (a) Hanabusa, K.; Tanaka, R.; Suzuki, M.; Kimura, M.; Shirai, H. *Adv. Mater.* **1997**, *9*, 1095−1097. (b) Bhattacharya, S.; Acharya, S. N. G.; Raju, A. R. *Chem. Commun.* **1996**, 2101−2102. (c) Bhattacharya, S.; Acharya, S. N. G. *Chem. Mater.* **1999**, *11*, 3121−3132.

(12) Shimizu, T.; Masuda, M. *J. Am. Chem. Soc.* **1997**, *119*, 2812−2818.

(13) Masuda, M.; Shimizu, T. *Carbohydr. Res.* **1997**, *302*, 139−147.

(14) Nezu, S.; Walsh, S.; Meille, V.; Yoshida, M.; Lando, J. B. *J. Polym. Sci., Part A: Polym. Chem.* **1995**, *33*, 973−977.

(15) (a) Masuda, M.; Shimizu, T. *Carbohydr. Res.* **2000**, *326*, 56−66. (b) Nakazawa, I.; Masuda, M.; Okada, Y.; Hanada, T.; Yase, K.; Asai, M.; Shimizu, T. *Langmuir* **1999**, *15*, 4757−4764.

(16) (a) Day, D.; Lando, J. B. *J. Polym. Sci., Polym. Lett. Ed.* **1981**, *19*, 227−233. (b) Rubner, M. F. *Macromolecules* **1986**, *19*, 2114−2128. (c) Perez, J.; Burillo, G.; Roa, M.; Vazquez, C.; Ogawa, T. *Polym. Bull.* **1992**, *27*, 527−534.

MA001157E